Available online at www.sciencedirect.com
ScienceDirect
Polymer 49 (2008) 1737–1742
polymer
www.elsevier.com/locate/polymer

Polymer Communication

Nanostructures and nanoporosity in thermoset epoxy blends with an amphiphilic polyisoprene-*block*-poly (4-vinyl pyridine) reactive diblock copolymer

Qipeng Guo [a,*], Jing Liu [a], Ling Chen [b], Ke Wang [b]

[a] *Centre for Material and Fibre Innovation, Deakin University, Pigdons Road, Geelong, Victoria 3217, Australia*
[b] *Institute of Materials Research and Engineering, 3 Research Link, Singapore 117602, Singapore*

Received 23 November 2007; received in revised form 16 February 2008; accepted 19 February 2008
Available online 23 February 2008

Abstract

Nanostructured thermoset blends were prepared based on a bisphenol A-type epoxy resin and an amphiphilic reactive diblock copolymer, namely polyisoprene-*block*-poly(4-vinyl pyridine) (PI-P4VP). Infrared spectra revealed that the P4VP block of the diblock copolymer reacted with the epoxy monomer. However, the non-reactive hydrophobic PI block of the diblock copolymer formed a separate microphase on the nanoscale. Ozone treatment was used to create nanoporosity in nanostructured epoxy/PI-P4VP blends via selective removal of the PI microphase and lead to nanoporous epoxy thermosets; disordered nanopores with the average diameter of about 60 nm were uniformly distributed in the blend with 50 wt% PI-P4VP. Multi-scale phase separation with a distinctly different morphology was observed at the air/sample interface due to the interfacial effects, whereas only uniform microphase separated morphology at the nanoscale was found in the bulk of the blend.

Keywords: Nanoporous epoxy; Thermoset blend; Block copolymer

1. Introduction

Epoxy resins are widely used as insulating and structural materials in manufacturing microelectronic devices and components such as computer chip packaging and circuit boards. Porous epoxy thermosets can reduce the dielectric constant by substitution of a portion of the matrix material with air. Reduced sizes in microelectronics have created a need for porosity at the nanometer scale in materials. However, porous epoxy thermosets achieved so far are generally with pore sizes larger than the submicron scale [1,2].

Nanostructured epoxy thermosets based on self-assembly of amphiphilic block copolymers have recently been explored in several laboratories [3–8]. Amphiphilic diblock copolymers containing poly(ethylene oxide) (PEO) blocks that are epoxy-miscible were employed to form well-defined ordered and disordered microstructures in thermoset epoxy resins by Bates and co-workers [3] and Mijovic et al. [4]. Guo and co-workers successfully prepared nanostructured thermoset epoxy resin blends with PEO-containing amphiphilic diblock, triblock and star-shaped block copolymers [5–8]. In addition, nanoscale structures can be created in epoxy blends with poly(ε-caprolactone) (PCL)-based block copolymers [9] and in crosslinked phenolic blends with amphiphilic block copolymers [10]. Nanostructured epoxy blends have also been obtained with ABC triblock copolymers [11,12] and reactive block copolymers, such as epoxidized polyisoprene–polybutadiene [13], epoxidized polystyrene–polybutadiene [14], glycidyl methacrylate-based [12,13,15] and methacrylic acid-based [12] block copolymers.

The formation of nanostructured thermoset epoxy/block copolymer blends means that nanoporous epoxy thermosets can be produced via subsequent removal of the degradable block. An effort has been paid to the creation and characterization of nanoporous epoxy thermosets via microphase separation of block copolymers in thermoset epoxies in this laboratory. We

* Corresponding author. Tel.: +61 3 5227 2802; fax: +61 3 5227 1103.
E-mail address: qguo@deakin.edu.au (Q. Guo).

0032-3861/$ - see front matter © 2008 Elsevier Ltd. All rights reserved.
doi:10.1016/j.polymer.2008.02.033

report here nanostructured thermoset blends of a bisphenol A-type epoxy resin (ER) and an amphiphilic reactive diblock copolymer, namely polyisoprene-*block*-poly(4-vinyl pyridine) (PI-P4VP). The P4VP block of the diblock copolymer can react with the epoxy monomer, while the non-reactive hydrophobic PI block of the diblock copolymer forms a separate microphase on the nanoscale. Ozone treatment was employed to create nanoporosity in nanostructured epoxy/PI-P4VP blends; nanoporous epoxy thermosets were produced by selective removal of the PI microphase in these blends.

2. Experimental

The amphiphilic PI-P4VP reactive diblock copolymer used was a product of Polymer Source, Inc., namely poly[isoprene (1,4 addition)-*b*-4-vinyl pyridine]. The diblock copolymer had a number-average molecular weight M_n of 41,700 with a polydispersity $M_w/M_n = 1.06$. The PI block had an $M_n = 30{,}000$; therefore, the weight fraction of the PI block was 0.72, corresponding to a PI volume fraction of approximately 0.75, on the basis of estimated densities [16]. The uncured epoxy resin, diglycidyl ether of bisphenol A (DGEBA), with $M_n = 340$ and the curing agent, 4,4′-methylenedianiline (MDA) were obtained from Aldrich Chemical Co., Inc. The uncured DGEBA/MDA/PI-P4VP blends were solvent-cast from well-dissolved 5% (w/v) solutions in chloroform at room temperature. Drying overnight at atmospheric pressure was followed by vacuum drying for 1 day. The stoichiometry was calculated to give a 1:1 ratio between the epoxy group and the sum of amine protons and pyridine nitrogens, that is, from MDA and the P4VP block of PI-P4VP, respectively. The blends were initially cured at 100 °C for 20 h and then postcured at 150 °C for 2 h and 175 °C for 1 h.

The ER/PI-P4VP blends were characterized using small-angle X-ray scattering (SAXS), atomic force microscopy (AFM), transmission electron microscopy (TEM), and attenuated total reflection Fourier transform infrared (ATR-FTIR) spectroscopy. AFM measurements were performed with a DME DS 45-40 scanning probe microscope (Denmark). Both the as-cured and ozone-treated samples were subjected for AFM observation. The specimens for TEM observation were cut at room temperature with a Leica Ultracut UCT ultramicrotome equipped with a diamond knife. The resulting ultrathin sections of 80 nm thickness of the ozone-treated specimens were picked up on copper grids and imaged with a Philips CM300 TEM at 300 kV in the bright-field mode. The SAXS measurements were performed with a Bruker NanoSTAR SAXS instrument at room temperature (25 °C) as described previously [7,8]. FTIR measurements were made with a Bruker Vertex 70 FT-IR spectrometer at room temperature at a resolution of 4 cm^{-1} using the cured blend samples with the air/sample interface.

3. Results and discussion

3.1. Nanostructures in epoxy/PI-P4VP blends

As P4VP homopolymer can cure epoxy resins [17], the curing reaction is expected to take place between the P4VP block and the epoxy precursor DGEBA. Obviously, this curing reaction would affect the phase behavior and morphology of the cured products; thus the chemical structure of the cured ER/PI-P4VP blends was investigated firstly.

Fig. 1 shows the ATR-FTIR spectra of the cured ER/PI-P4VP blends with different compositions. It can be seen that the characteristic bands of infrared absorption of these samples change with increasing PI-P4VP content. The noticeable absorption band changes take place at 2963, 2928, 1642, 1450 and 1375 cm^{-1} wavenumbers (as denoted in Fig. 1). The intensities grow in these positions as the concentration of PI-P4VP in the blend is increased. It is known that the bands at 2963 and 2928 cm^{-1} can be attributed to the C–H stretching of $-CH_3$ group and the asymmetric stretching of $-CH_2-$ group, respectively [18,19]. Therefore, for the high contents of methyl and methylene in the PI blocks, the intensities in these bands increase with increasing PI amount, i.e., block copolymer in the blends. Meanwhile, the band at 1450 cm^{-1}, which is attributed to the bending vibration of $-CH_3$ group, together with that at 1375 cm^{-1}, which is due to methyl asymmetric deformation vibration of PI [18,19], also increase with the content of PI-P4VP block copolymer.

It is anticipated that the pyridine ring in the P4VP blocks may participate in the curing reaction with DGEBA as the additional curing agent other than MDA. The reaction between P4VP blocks and DGEBA improves the miscibility of the P4VP blocks with the cured ER. To some extent, via the curing, the reacted P4VP becomes a part of the epoxy thermosets through the linking of chemical bonds.

From the infrared spectra of the cured blends in Fig. 1, the reaction between the pyridine rings and DGEBA is verified. The new band at 1642 cm^{-1} for the cured blends does not belong to any characteristic absorption bands of the epoxy precursor DGEBA, curing agent MDA or PI-P4VP. Therefore it should be related with the new chemical structure formed during the curing process, i.e., the unconjugated carbon double bonds which resulted from the reaction of pyridine ring and DGEBA [17]. Meanwhile, it is also found that the intensity of this new band increases with PI-P4VP content, which further demonstrates the relationship between this band and the reaction of P4VP blocks and DGEBA.

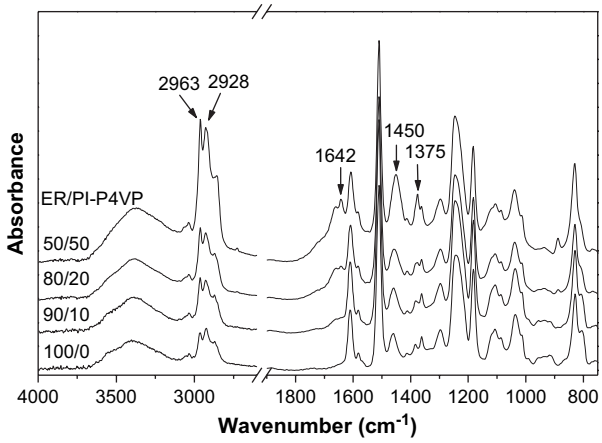

Fig. 1. ATR-FTIR spectra in the range of 4000–750 cm^{-1} for 100/0, 90/10, 80/20 and 50/50 ER/PI-P4VP blends.

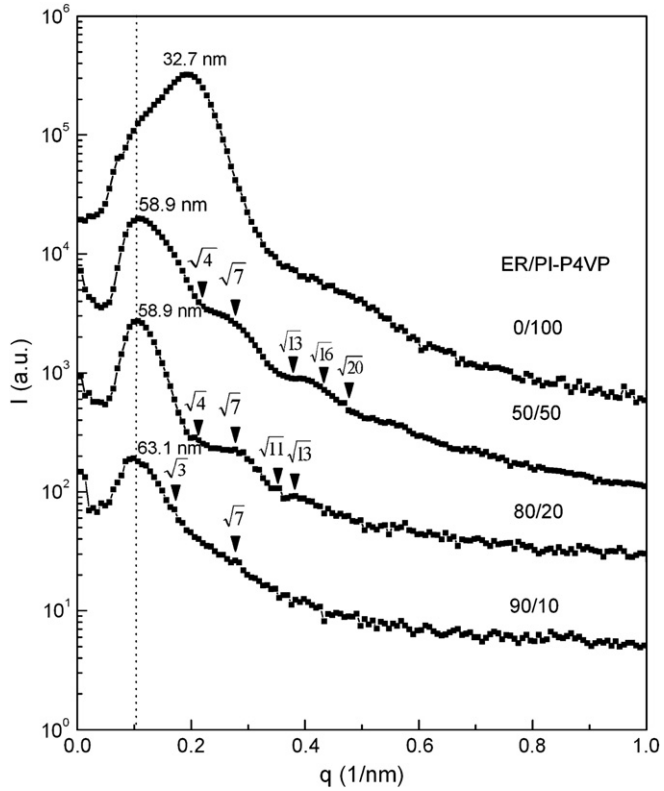

Fig. 2. SAXS patterns of ER/PI-P4VP blends at room temperature (25 °C). The scattering vector $q = (4\pi/\lambda)\sin(\theta/2)$, where $\lambda = 0.154$ nm is the wavelength and θ the scattering angle.

From the above analysis of the chemical structure of the cured blends, it is clear that the P4VP chain segments were involved in the cure reaction with DGEBA. Meanwhile, the weak polarity of the PI block indicates its immiscibility with both the epoxy resin and the P4VP block. Consequently, microphase separation took place in this blends system.

The morphology of cured blends with different contents of the copolymer was investigated by SAXS technique. The SAXS profiles are shown in Fig. 2. For the plain PI-P4VP copolymer (the top one in Fig. 2), a broad first-order scattering maximum at $q = 0.19$ and a shoulder around $q = 0.47$ are detected. From the relative intensities and shapes of the first-order and shoulder peaks, it can be concluded that the block copolymer forms disordered spherical microdomains by microphase separation. The average distance between the microdomains is 32.7 nm. For the ER/PI-P4VP blends, a scattering peak corresponding to a space of 58.9 nm is observed in the figure for blends with 20 and 50 wt% PI-P4VP. Meanwhile, a space of 63.1 nm in the blend with 10 wt% PI-P4VP is obtained from the position of the first-order peak. Furthermore, some weak and broad peaks also appear in the profiles besides the first-order peaks. Though some positions of the peaks match the characters of hexagonally-packed cylindrical morphology, i.e., $q/q^* = 1 : \sqrt{3} : \sqrt{4} : \sqrt{7} : \sqrt{9} : \sqrt{12} : \sqrt{13}$ (where q^* denotes the position of the first-order scattering maximum), it is difficult to deduce that there are long-range ordered structures in the blends due to the weakness and broadness of these peaks in the profiles [20–25]. The occurrence of cure reaction affected the phase behavior and destroyed any long-range ordered structures, but led to the formation of new microphase separated structures. Some of the short-range ordered morphology in the uncured blend samples was fixed by the formation of epoxy crosslinking network.

Consequently, from the whole shapes of the SAXS profiles in Fig. 2, it can be concluded that there exists only short-range ordered nanostructures in the cured ER/PI-P4VP blends. However, fairly uniform microdomain sizes in the cured blends were verified by TEM observations after ozonolysis, which will be discussed in the following part.

The morphology at the air/sample interface of cured ER/PI-P4VP blend sample with 50 wt% PI-P4VP was also investigated. As it is known, for the interfacial effects, many properties of material will change at the interface, such as the glass transition temperature, crystallization rate, etc. [26–32]. For the present blend sample, from the AFM results in Fig. 3, especially from the phase image on the right, it can be seen that multi-scale phase separation took place at the air/sample interface of cured ER/PI-P4VP, including spherical microdomains and irregular areas. The size of microdomains is in the range from around several tens of nanometers to approximately 1 μm. In the blend surface, due to the additional driving force of lowering surface free energy,

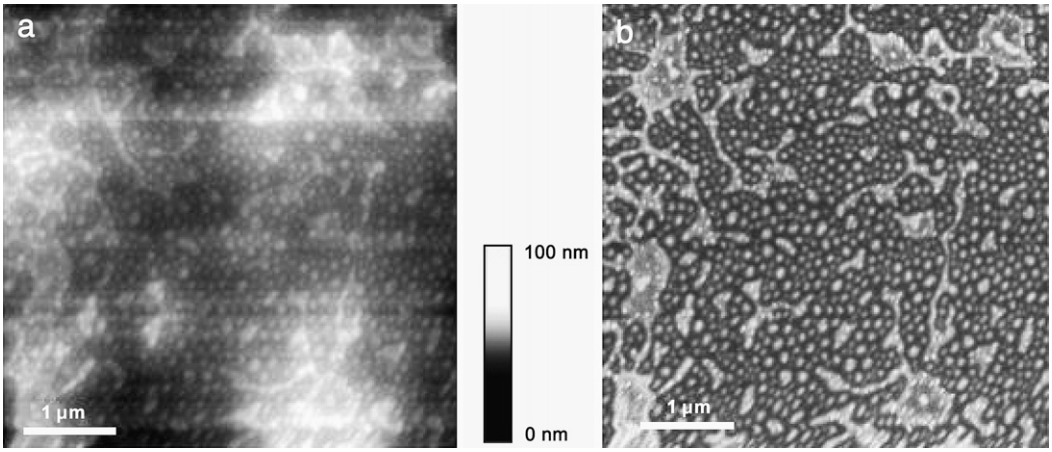

Fig. 3. AFM image of 50/50 ER/PI-P4VP blend at the air/sample interface before ozonolysis: (a) height image and (b) phase image.

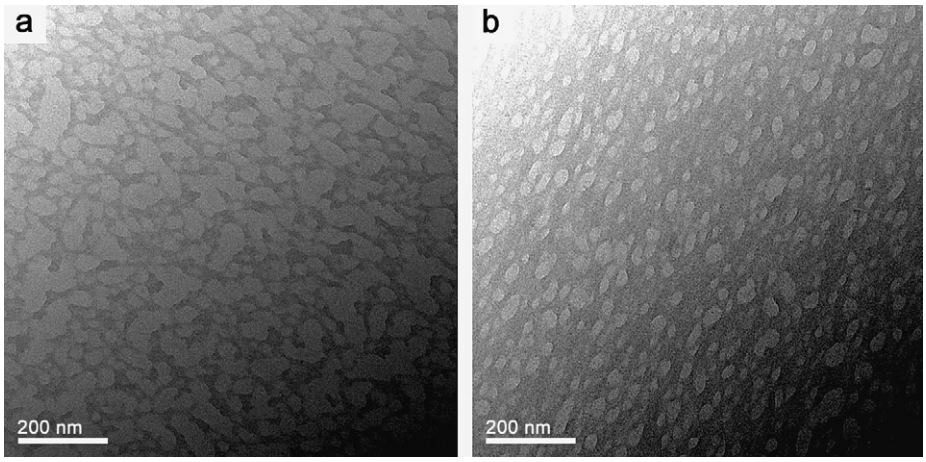

Fig. 4. TEM micrographs of (a) 80/20 and (b) 50/50 ER/PI-P4VP blends. The specimens were treated with ozone for 24 h to remove the PI microphase.

the phase separation process was significantly influenced. Therefore, the morphology at the interface is remarkably different from that in the bulk of the blend where only uniform microphase separation and microdomains in the same size range were observed as will be seen below. In view of the large difference in polarity between the PI block and the other components (the P4VP block and the epoxy precursor DGEBA) of the blends, microphase separation of the PI block could take place at the early stage of processing, even before the chloroform had finally been vaporized. This would also affect the formation of a distinctly different morphology at the air/sample interface that was eventually formed.

3.2. Creation of nanoporosity in epoxy/PI-P4VP blends via ozonolysis

To discern the microphase of PI blocks and create nanoporous structure in the ER/PI-P4VP blends, ozonolysis was used to selectively degrade the PI block of PI-P4VP in the blends. The blend films of about 1 mm thick were soaked in water and ozone was bubbled in the aqueous solution for 24 h at room temperature; the cleaved compounds were leached out from the films.

Fig. 4 shows TEM images of nanoporous epoxy thermosets created by the selective removal of PI microphase in the cured ER/PI-P4VP blends. The disordered, fairly uniform nanoporous structures can be seen in the blends with 20 and 50 wt% PI-P4VP. The sizes of the nanopores are mainly in the range of several tens of nanometers, which matches the SAXS results well. Meanwhile, the microphase of PI blocks is also discerned by the TEM results, corresponding to the nanopores after ozonolysis. For the blends with 50 wt% PI-P4VP, the cured ER containing reacted P4VP blocks forms the main continuous phase, while PI blocks compose the spherical microdomains with the average size about 60 nm (the white areas in Fig. 4b) and all distributed disorderedly in the ER continuous phase in diameter (the dark areas). It can also be found that the composition of the blends has an important effect on the morphology. The cured ER with 20 wt% PI-P4VP (Fig. 4a) exhibits some characteristics of bicontinuous phase structure, remarkably different from that of 50 wt% copolymer (Fig. 4b).

The TEM results reveal the uniform nanostructures of the bulk blend samples. Meanwhile, the microphase morphology at the air/sample interface of the same blend was studied by AFM. The AFM images are shown in Fig. 5. By comparing the AFM images before (Fig. 3) and after (Fig. 5) ozonolysis, the morphology difference can be clearly seen. It is noticed

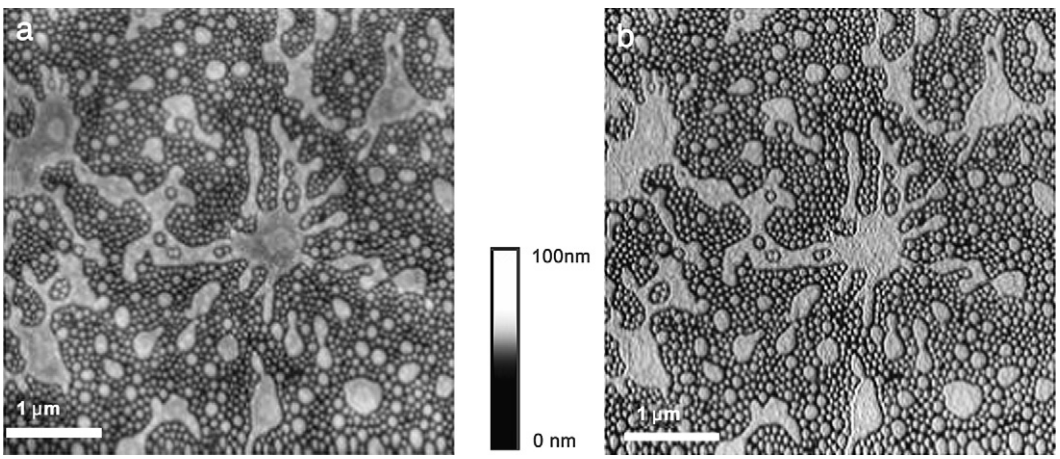

Fig. 5. AFM image of 50/50 ER/PI-P4VP blend at the air/sample interface after ozonolysis for 60 min: (a) height image and (b) phase image.

from Fig. 5 that the appearance of the spherical microdomains (the bright areas) is much clearer after ozonolysis. The dark surrounding areas show the regions where the PI microphase was removed by ozonolysis (Fig. 5). It seems that some other spherical microdomains hiding behind the "dark" substance were revealed by ozonolysis. It is known that the PI homopolymer possesses a glass transition temperature of about −60 °C [33], which is much lower than those of cured ER containing P4VP blocks and the P4VP block itself. Therefore, the PI microphase is a "soft" phase compared with other components in the blends. Furthermore, the PI is the only component that can be degraded by ozonolysis in the blends system. So the appearance of dark surrounding areas indicates the degradation and removal of the PI blocks.

Consequently, the phase separated structure at the interface can be described as follows: phase separation took place at the interface on multi-scales; the ER phase is found in both the large scale of the micrometer size and the spherical microdomains with the diameters in the several tens of nanometers; P4VP blocks of the PI-P4VP mainly coexist with the cured ER in the spherical microdomains while the PI blocks are separated, surrounding the spherical microdomains, owing to their weak polarity and immiscibility with other components.

It is interesting to notice the difference between the phase structures at the interface and in the bulk of the same blend. Firstly, the phase separation took place on multi-scales at the interface while only uniform microphase separation occurred in the bulk of the blend. Secondly, the spherical microdomains at the interface are composed of the cured ER containing P4VP blocks; the PI blocks surround the spherical microdomains. In the bulk sample the spherical microdomains consisting of PI blocks and the cured ER constitutes the continuous phase.

The change in chemical structure after ozonolysis was recorded by the ATR-FTIR method. As displayed in Fig. 6, the bands with significant difference after the ozonolysis are found at the positions of 2963, 2928 and 2857 and 1450 cm^{-1}. The intensities of all these bands decrease after ozonolysis.

The band at 2963 is related to the C−H stretching of $-CH_3$ group; the bands at 2928 and 2857 cm^{-1} are assigned to the asymmetric and symmetric stretching of $-CH_2-$ group, respectively. Besides, the absorption at 1450 cm^{-1} is assigned to the bending vibration of $-CH_3$ group. The obvious decrease in the intensities of these bands indicates a drop in the amounts of $-CH_3$ and $-CH_2-$ groups in the cured blends after ozonolysis. This comes from the degradation of PI blocks via ozonolysis, where the double bonds were broken and the $-CH_3$ and $-CH_2-$ groups of the PI blocks are peeled away. So the contents of $-CH_3$ and $-CH_2-$ groups in the blends are impaired and the corresponding infrared absorptions decrease.

The ATR-FTIR results further verify that the dark areas surrounding the bright spherical microdomains in the AFM images (Fig. 5b) indicate the disappeared PI microphase. The ozonolysis method is an efficient way to remove the PI component from the nanostructured blends and create nanoporosity in the cured ER blends.

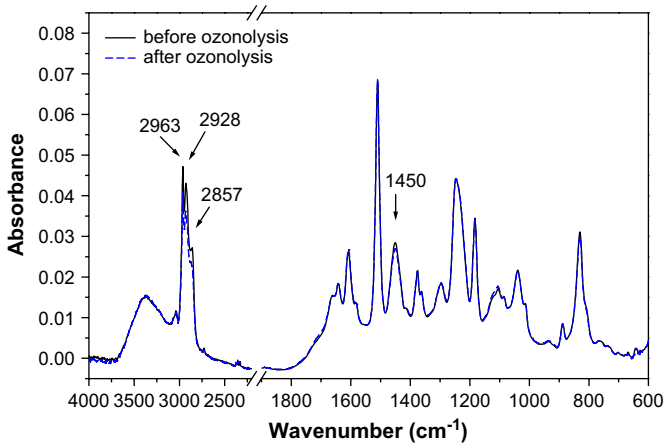

Fig. 6. ATR-FTIR spectra in the range of 4000−600 cm^{-1} for 50/50 ER/PI-P4VP blend before and after ozonolysis.

4. Conclusion

In conclusion, we have successfully prepared nanostructured epoxy/PI-P4VP blends via microphase separation of PI-P4VP block copolymer. Nanoporosity can be created in the nanostructured epoxy/PI-P4VP blends via ozonolysis method. Infrared spectra showed that the P4VP block also acted as the additional curing agent in this system during the curing process. Disordered nanopores with the average diameter of about 60 nm were uniformly distributed in the cured blend with 50 wt% PI-P4VP. Multi-scale phase separation with a distinctly different morphology was observed at the air/sample interface due to the interfacial effects, whereas only uniform microphase separation on the nanoscale was found in the bulk of the blend.

Acknowledgments

One of us (Q.G.) would like to express his gratitude to the Australian Research Council for financial support under the Discovery Projects Scheme.

References

[1] Khemani KC, editor. Polymeric foams: science and technology. Washington DC: ACS; 1997.
[2] Klempner DC, Frisch KC, editors. Handbook of polymeric foams and technology. Munich: Hanser; 1991.
[3] (a) Hillmyer MA, Lipic PM, Hajduk DA, Almdal K, Bates FS. J Am Chem Soc 1997;119:2749;
(b) Lipic PM, Bates FS, Hillmyer MA. J Am Chem Soc 1998;120:8963.
[4] Mijovic JS, Shen M, Sy JW, Mondragon I. Macromolecules 2000;33:5235.
[5] Guo Q, Thomann R, Gronski W, Thurn-Albrecht T. Macromolecules 2002;35:3133.
[6] Guo Q, Thomann R, Gronski W, Staneva R, Ivanova R, Stühn B. Macromolecules 2003;36:3635.
[7] Guo Q, Wang K, Chen L, Zheng S, Halley PJ. J Polym Sci Part B Polym Phys 2006;44:975.
[8] Guo Q, Chen F, Wang K, Chen L. J Polym Sci Part B Polym Phys 2006;44:3042.
[9] Meng F, Zheng S, Zhang W, Li H, Liang Q. Macromolecules 2006;39:711.

[10] (a) Kosonen H, Ruokolainen J, Nyholm P, Ikkala O. Macromolecules 2001;34:3046;
(b) Kosonen H, Ruokolainen J, Nyholm P, Ikkala O. Polymer 2001;42:9481;
(c) Kosonen H, Ruokolainen J, Torkkeli M, Serimaa R, Nyholm P, Ikkala O. Macromol Chem Phys 2002;203:388.
[11] (a) Ritzenthaler S, Court F, David L, Girard-Reydet E, Leibler L, Pascault JP. Macromolecules 2002;35:6245;
(b) Ritzenthaler S, Court F, Girard-Reydet E, Leibler L, Pascault JP. Macromolecules 2003;36:118;
(c) Girard-Reydet E, Pascault JP, Bonnet A, Court F, Leibler L. Macromol Symp 2003;198:309.
[12] (a) Rebizant V, Abetz V, Tournilhac F, Court F, Leibler L. Macromolecules 2003;36:9889;
(b) Rebizant V, Venet AS, Tournilhac F, Girard-Reydet E, Navarro C, Pascault JP, et al. Macromolecules 2004;37:8017.
[13] Grubbs RB, Broz ME, Dean JM, Bates FS. Macromolecules 2000;33:2308. 9522; 2001; 34: 8593.
[14] (a) Serrano E, Martin MD, Tercjak A, Pomposo JA, Mecerreyes D, Mondragon I. Macromol Rapid Commun 2005;26:982;
(b) Macromol Chem Phys 2004;205:987.
[15] Guo Q, Dean JM, Grubbs RB, Bates FS. J Polym Sci Part B Polym Phys 1994;2003:41.
[16] Sewell JH. J Appl Polym Sci 1973;17:1741.
[17] Meng F, Zhang W, Zheng S. J Mater Sci 2005;40:6367.
[18] dos Santos KAM, Suarez PAZ, Rubim JC. Polym Degrad Stab 2005;90:34.
[19] Dasgupta S, Pande JB, Ramakrishnan CS. J Polym Sci 1955;17:255.
[20] Hamley IW, Fairclough JPA, Ryan AJ, Bates FS, Towns-Andrews E. Polymer 1996;37:4425.
[21] Nojima S, Hashizume K, Rohadi A, Sasaki S. Polymer 1997;38:2711.
[22] Park C, Simmons S, Fetters LJ, Hsiao B, Yeh F, Thomas EL. Polymer 2000;41:2971.
[23] Tsubaki K, Ishizu K. Polymer 2001;42:8387.
[24] Sun L, Liu YX, Zhu L, Hsiao BS, Avila-Orta CA. Polymer 2004;45:8181.
[25] Bondzic S, Polushkin E, Schouten AJ, Ikkala O, ten Brinke G. Polymer 2007;48:4723.
[26] Tan NCB, Wu WL, Wallace WE, Davis GT. J Polym Sci Part B Polym Phys 1998;36:155.
[27] Fryer DS, Nealey PF, de Pablo JJ. Macromolecules 2000;33:6439.
[28] Dalnoki-Veress K, Forrest JA, Massa MV, Pratt A, Williams A. J Polym Sci Part B Polym Phys 2001;39:2615.
[29] Sills S, Overney RM, Chau W, Lee VY, Miller RD, Frommer J. J Chem Phys 2004;120:5334.
[30] Akabori K, Tanaka K, Nagamura T, Takahara A, Kajiyama T. Macromolecules 2005;38:9735.
[31] Vogt BD, Soles CL, Lee HJ, Lin EK, Wu WL. Polymer 2005;46:1635.
[32] Zhang Y, Mukoyama S, Hu Y, Yan C, Ozaki Y, Takahashi I. Macromolecules 2007;40:4009.
[33] Wang J, Roland CM. Polymer 2005;46:4160.